Supplemental Data

Data analysis

Estimation of individual contribution of CYP1A1 and CYP1A2 to EROD and MROD in liver microsomes from TCDD-treated hCYP1A1/1A2 mice

Data were analysed by simultaneous non-linear regression analysis (Kakkar et al., 1999; Kakkar et al., 2000) using GraFit 7.0.3 (Erithacus Software Limited, UK). Complete data set for EROD by recombinant human CYP1A1 (with and without quinidine) was fitted simultaneously using mixed, non-competitive, competitive and uncompetitive inhibition models with substrate inhibition. ER and quinidine concentrations were two independent variables in the corresponding equations for the simultaneous non-linear regression. Fits produced by different inhibition models were compared using QuickCalcs online application (GraphPad software, USA; http://graphpad.com/quickcalcs/aic1/). The most statistically preferable model for the inhibition of EROD metabolism catalysed by recombinant CYP1A1 in the presence of quinidine was mixed inhibition with substrate inhibition (**Eq. 1**; **Scheme 1a**):

$$v_{EROD;CYP1A1} = \frac{[S]*V_{max}}{\left(1+\frac{[I]}{K_i}\right)*K_{S1}+\left(1+\frac{[S]}{K_{S2}}+\frac{[I]}{\alpha*K_i}\right)*[S]} \qquad \textbf{Eq. 1}$$

Where $v_{EROD;CYP1A1}$ is the EROD reaction rate catalysed by CYP1A1; [S] is the concentration of ER; V_{max} is the reaction rate at infinite substrate concentration in the absence of an inhibitor and substrate inhibition; [I] is the concentration of CYP1A1 inhibitor quinidine; K_i is a dissociation constant of the enzyme-inhibitor complex; K_{s1} is a dissociation constant of the productive enzyme-substrate complex; K_{s2} is a dissociation constant of the inhibitory enzyme-substrate complex and α is a parameter describing the effect of inhibitor binding on the binding of the substrate and *vice versa*. EROD activity by recombinant human CYP1A2 was not affected by quinidine, so the reaction rate dependency from ER concentration was analysed using Michaelis-

Menten equation (**Eq. 2**; **Scheme 1b**).

$$v_{EROD;CYP1A2} = \frac{[S]*V_{max}}{K_m+[S]} \quad \textbf{Eq. 2}$$

Where $v_{EROD;CYP1A2}$ is the EROD reaction rate catalysed by CYP1A2; [S] is concentration of ER; V_{max} is reaction rate at infinite substrate concentration; K_m is Michaelis constant.

EROD activity in liver microsomes from TCDD-treated Cyp1a KO mice was weakly inhibited by quinidine. Non-competitive inhibition with substrate inhibition gave the statistically best fit (**Eq. 3**; **Scheme 1c**).

$$v_{EROD;Non-CYP1A} = \frac{[S]*V_{max}}{\left(1+\frac{[I]}{K_i}\right)*K_{S1}+\left(1+\frac{[S]}{K_{S2}}+\frac{[I]}{K_i}\right)*[S]} \quad \textbf{Eq. 3}$$

Where $v_{EROD;Non-CYP1A}$ is the EROD reaction rate catalysed by cytochromes P450 other than CYP1A; [S] is concentration of ER; V_{max} is the reaction rate at infinite substrate concentration in the absence of an inhibitor and substrate inhibition; [I] is concentration of quinidine; K_i is a dissociation constant of the enzyme-inhibitor complex; K_{s1} is a dissociation constant of the productive enzyme-substrate complex and K_{s2} is a dissociation constant of the inhibitory enzyme-substrate complex.

For inhibition by quinidine of MROD activity catalysed by recombinant human CYP1A1 the statistically best fit was a competitive mechanism with substrate inhibition (**Eq. 4**; **Scheme 1d**).

$$v_{MROD;CYP1A1} = \frac{[S]*V_{max}}{\left(1+\frac{[I]}{K_i}\right)*K_{S1}+\left(1+\frac{[S]}{K_{S2}}\right)*[S]} \quad \textbf{Eq. 4}$$

Where $v_{MROD;CYP1A1}$ is the MROD reaction rate catalysed by CYP1A1; [S] is the concentration of MR; V_{max} is the reaction rate at infinite substrate concentration in the absence of an inhibitor and substrate inhibition; [I] is the concentration of CYP1A1 inhibitor quinidine; K_i is a dissociation constant of the enzyme-inhibitor complex; K_{s1} is a dissociation constant of the productive enzyme-substrate complex and K_{s2} is a

dissociation constant of the inhibitory enzyme-substrate complex.

Quinidine did not affect MROD activity when catalysed by CYP1A2, so the reaction rate versus MR concentration dependency was fitted using equation for saturation kinetics with substrate inhibition (**Eq. 5**; **Scheme 1e**).

$$v_{MROD;CYP1A2} = \frac{[S]*V_{max}}{K_{S1}+\left(1+\frac{[S]}{K_{S2}}\right)*[S]} \quad \textbf{Eq. 5}$$

Where $v_{MROD;CYP1A2}$ is the MROD reaction rate catalysed by CYP1A2; [S] is the concentration of MR; V_{max} is the reaction rate at infinite substrate concentration in the absence of substrate inhibition; K_{s1} is a dissociation constant of the productive enzyme-substrate complex and K_{s2} is a dissociation constant of the inhibitory enzyme-substrate complex.

Kinetics of MROD inhibition by quinidine in liver microsomes from TCDD-treated Cyp1a KO mice was best described by the non-competitive inhibition with substrate inhibition in which the enzyme can bind simultaneously two substrate molecules (one in productive and one in the inhibition orientation) and one molecule of quinidine (**Eq. 6**; **Scheme 1f**).

$$v_{MROD;Non-CYP1A} = \frac{[S]*V_{max}}{\left(1+\frac{[I]}{K_i}\right)*K_{S1}+\left(1+\frac{[I]}{K_i}+\frac{[S]}{K_{S2}}*\left(1+\frac{[I]}{K_i}\right)\right)*[S]} \quad \textbf{Eq. 6}$$

Where $v_{MROD;CYP1A1}$ is the MROD reaction rate catalysed by cytochromes P450 other than CYP1A; [S] is concentration of MR; V_{max} is the reaction rate at infinite substrate concentration in the absence of an inhibitor and substrate inhibition; [I] is the concentration of quinidine; K_i is a dissociation constant of the enzyme-inhibitor complex; K_{s1} is a dissociation constant of the productive enzyme-substrate complex and K_{s2} is a dissociation constant of the inhibitory enzyme-substrate complex.

In liver microsomes from TCDD-treated hCYP1A1/1A2 mice, EROD and MROD activities were assumed to be catalysed by three components, namely human CYP1A1, human CYP1A2 and a non-Cyp1a component. Substrate kinetics, inhibition

mechanism and values of the substrate and quinidine binding constants for each component were obtained in the experiments with recombinant enzymes and liver microsomes from TCDD-treated Cyp1a KO mice (**Supplementary Table 1**). Thus, for liver microsomes from TCDD-treated hCYP1A1/1A2 mice, dependency of the EROD or MROD reaction rate versus substrate and quinidine concentration can be presented as a sum of the reaction rates of the above three individual components (**Eq. 7-8**).

$$v_{EROD;hCYP1A1/1A2} = v_{EROD;CYP1A1} + v_{EROD;CYP1A2} + v_{EROD;Non-CYP1A} = \\ = \frac{[S]*V_{maxCYP1A1}}{\left(1+\frac{[I]}{3.3}\right)*0.09+\left(1+\frac{[S]}{11}+\frac{[I]}{31*3.3}\right)*[S]} + \frac{[S]*V_{maxCYP1A2}}{1.2+[S]} + \frac{[S]*214}{\left(1+\frac{[I]}{422}\right)*0.83+\left(1+\frac{[S]}{13}+\frac{[I]}{422}\right)*[S]} \quad \textbf{Eq. 7}$$

Where $v_{EROD;hCYP1A1/1A2}$ is the total EROD reaction rate in hCYP1A1/1A2 liver microsomes from TCDD-treated mice; $v_{EROD;CYP1A1}$ is the EROD reaction rate catalysed by CYP1A1; $v_{EROD;CYP1A2}$ is the EROD reaction rate catalysed by CYP1A2; $v_{EROD;Non-CYP1A}$ is the EROD reaction rate catalysed by hCYP1A1/1A2 mouse cytochromes P450 other than CYP1A; [S] is the concentration of ER; [I] is the concentration of quinidine; $V_{maxCYP1A1}$ is the reaction rate catalysed by CYP1A1 component of the hCYP1A1/1A2 liver microsomes from TCDD-treated mice at infinite substrate concentration and in the absence of an inhibitor and substrate inhibition and $V_{maxCYP1A2}$ is the reaction rate catalysed by CYP1A2 component of hCYP1A1/1A2 liver microsomes from TCDD treated mice at the infinite substrate concentration.

$$v_{MROD;hCYP1A1/1A2} = v_{MROD;CYP1A1} + v_{MROD;CYP1A2} + v_{MROD;Non-CYP1A} = \\ = \frac{[S]*V_{maxCYP1A1}}{\left(1+\frac{[I]}{2.2}\right)*0.47+\left(1+\frac{[S]}{1.3}\right)*[S]} + \frac{[S]*V_{maxCYP1A2}}{0.58+\left(1+\frac{[S]}{12}\right)*[S]} + \frac{[S]*58}{\left(1+\frac{[I]}{272}\right)*0.96+\left(1+\frac{[I]}{272}+\frac{[S]}{3.4}*\left(1+\frac{[I]}{272}\right)\right)*[S]} \quad \textbf{Eq. 8}$$

Where $v_{MROD;hCYP1A1/1A2}$ is the total MROD reaction rate in hCYP1A1/1A2 liver microsomes from TCDD treated mice; $v_{MROD;CYP1A1}$ is the MROD reaction rate catalysed by CYP1A1; $v_{MROD;CYP1A2}$ is the MROD reaction rate catalysed by CYP1A2; $v_{MROD;Non-CYP1A}$ is the MROD reaction rate catalysed by hCYP1A1/1A2 mouse cytochromes P450 other than CYP1A; [S] is the concentration of MR; [I] is the concentration of quinidine; $V_{maxCYP1A1}$ is the reaction rate catalysed by CYP1A1

component of the hCYP1A1/1A2 liver microsomes from TCDD treated mice at infinite substrate concentration and in the absence of an inhibitor and substrate inhibition and $V_{maxCYP1A2}$ is the reaction rate catalysed by CYP1A2 component of hCYP1A1/1A2 liver microsomes from TCDD-treated mice at the infinite substrate concentration and in the absence of substrate inhibition.

Substrate and quinidine concentrations are two independent variables in the equations, whilst V_{max}(CYP1A1) and V_{max}(CYP1A2) are two parameters which were calculated by non-linear regression analysis of the quinidine inhibition of EROD and MROD in TCDD treated hCYP1A1/1A2 liver microsomes using Equation 7 and Equation 8 respectively. Values of V_{max}(CYP1A1) and V_{max}(CYP1A2) for each reaction together with previously obtained values of substrate and quinidine binding constants allowed calculation of the EROD or MROD reaction rate in hCYP1A1/1A2 liver microsomes individually for the CYP1A1, CYP1A2 and Cyp1a KO components for any substrate or inhibitor concentration. This then allowed the calculation of the contribution of each individual catalytic component (**Eq. 9-14**).

$$Contr_{EROD;CYP1A1} = \frac{v_{EROD;CYP1A1}*100}{v_{EROD;hCYP1A1/1A2}} \quad \textbf{Eq. 9}$$

where $Contr_{EROD;CYP1A1}$ is th erelative contribution of human CYP1A1 to EROD; $v_{EROD;CYP1A1}$ is the EROD reaction rate catalysed by human CYP1A1 and $v_{EROD;hCYP1A1/1A2}$ is the total EROD reaction rate at given substrate and inhibitor concentrations.

$$Contr_{EROD;CYP1A2} = \frac{v_{EROD;CYP1A2}*100}{v_{EROD;hCYP1A1/1A2}} \quad \textbf{Eq. 10}$$

Where $Contr_{EROD;CYP1A2}$ is the relative contribution of human CYP1A2 to EROD; $v_{EROD;CYP1A2}$ is the EROD reaction rate catalysed by human CYP1A2 and $v_{EROD;hCYP1A1/1A2}$ is the total EROD reaction rate at given substrate and inhibitor concentrations.

$$Contr_{EROD;Non-CYP1A} = \frac{v_{EROD;Non-CYP1A2}*100}{v_{EROD;hCYP1A1/1A2}}$$ **Eq. 11**

Where $Contr_{EROD;Non-CYP1A}$ is the relative contribution of cytochromes P450 other than human CYP1A to EROD; $v_{EROD;\ Non-CYP1A}$ is the EROD reaction rate catalysed by cytochromes P450 other than human CYP1A and $v_{EROD;hCYP1A1/1A2}$ is the total EROD reaction rate at given substrate and inhibitor concentrations.

$$Contr_{MROD;CYP1A1} = \frac{v_{MROD;CYP1A1}*100}{v_{MROD;hCYP1A1/1A2}}$$ **Eq. 12**

Where $Contr_{MROD;CYP1A1}$ is the relative contribution of human CYP1A1 to MROD; $v_{MROD;CYP1A1}$ is the MROD reaction rate catalysed by human CYP1A1 and $v_{MROD;hCYP1A1/1A2}$ is the total MROD reaction rate at given substrate and inhibitor concentrations.

$$Contr_{MROD;CYP1A2} = \frac{v_{MROD;CYP1A2}*100}{v_{MROD;hCYP1A1/1A2}}$$ **Eq. 13**

Where $Contr_{MROD;CYP1A2}$ is the relative contribution of human CYP1A2 to MROD; $v_{MROD;CYP1A2}$ is the MROD reaction rate catalysed by human CYP1A2 and $v_{MROD;hCYP1A1/1A2}$ is the total EROD reaction rate at given substrate and inhibitor concentrations.

$$Contr_{MROD;Non-CYP1A} = \frac{v_{MROD;Non-CYP1A2}*100}{v_{MROD;hCYP1A1/1A2}}$$ **Eq. 14**

Where $Contr_{MROD;Non-CYP1A}$ is the relative contribution of cytochromes P450 other than human CYP1A to MROD; $v_{MROD;\ Non-CYP1A}$ is the MROD reaction rate catalysed by cytochromes P450 other than human CYP1A and $v_{MROD;hCYP1A1/1A2}$ is the total MROD reaction rate at given substrate and inhibitor concentrations.

Calculation of ramelteon and tacrine *in vitro* clearance and their fraction metabolised by Cyp1a2 and CYP1A2

For each microsomal preparation, the time course of substrate depletion was analysed by non-compartmental analysis using Phoenix WinNonlin version 6.4 (Certara, St. Louis, USA). The model type was Plasma (200-202) and the dose option was IV Bolus.

Clearance was calculated by dividing the dose (0.001 μmol; amount of the compound in 1 ml of the reaction mixture) by AUCinf_pred and amount of the microsomal protein in 1 ml of the reaction mixture. The fraction metabolised by Cyp1a2 and CYP1A2 for both compounds was calculated using **Eq. 15** and **Eq. 16**, respectively:

$$fm_{Cyp1a2} = \frac{CL_{in\ vitro(WT)} - CL_{in\ vitro(Cyp1a\ KO)}}{CL_{in\ vitro(WT)}} \quad \textbf{Eq. 15}$$

Where fm_{Cyp1a2} is a fraction of compound metabolised by Cyp1a2; $CL_{in\_vitro(WT)}$ and $CL_{in\_vitro(Cyp1a\ KO)}$ are the *in vitro* clearances of the compound in microsomes from WT and Cyp1a KO mice, respectively

$$fm_{CYP1A2} = \frac{CL_{in\ vitro(hCYP1A1/1A2)} - CL_{in\ vitro(Cyp1a\ KO)}}{CL_{in\ vitro(hCYP1A1/1A2)}} \quad \textbf{Eq. 16}$$

Where fm_{CYP1A2} is a fraction of compound metabolised by CYP1A2; $CL_{in\_vitro(hCYP1A1/1A2)}$ and $CL_{in\_vitro(Cyp1a\ KO)}$ are the *in vitro* clearances of the compound in microsomes from hCYP1A1/1A2 and Cyp1a KO mice, respectively

Extrapolation of caffeine PK to man

The time courses of caffeine concentration in hCYP1A1/1A2, Cyp1a KO and HRN mice were extrapolated to those in man using the complex Dedrick plot approach (Gabrielsson and Weiner, 2006). The bioavailability of caffeine is 1 in both man and mice. It distributes into the total body water, which makes caffeine concentration and clearance in whole blood equal to those in plasma (Bonati et al., 1984). Slopes for human to mouse allometric plots for volume of distribution and clearance were calculated using Eq. 17 and Eq. 18 respectively; human body weight, caffeine volume of distribution and clearance in man were assumed to be 82 kg, 40L and 0.105 L/min respectively (Culm-Merdek et al., 2005). Values for mouse body weight (0.0329 kg), caffeine volume of distribution (0.036 L) and clearance (0.000337 L/min) were those measured in hCYP1A1/1A2 mice.

$$d = \frac{\ln(V_{hCYP1A1/1A2}) - \ln(V_{Man})}{\ln(BW_{hCYP1A1/1A2}) - \ln(BW_{Man})}$$ **Eq. 17**

Where d is a slope of allometric plot for caffeine volume of distribution; $V_{hCYP1A1/1A2}$ and V_{Man} are caffeine volumes of distribution in humanised mice and human respectively; $BW_{hCYP1A1/1A2}$ and BW_{Man} are body weights of humanised mice and human respectively

$$b = \frac{\ln(CL_{hCYP1A1/1A2}) - \ln(CL_{Man})}{\ln(BW_{hCYP1A1/1A2}) - \ln(BW_{Man})}$$ **Eq. 18**

Where b is a slope of allometric plot for caffeine clearance; $CL_{hCYP1A1/1A2}$ and CL_{Man} are caffeine oral clearances in humanised mice and human respectively; $BW_{hCYP1A1/1A2}$ and BW_{Man} are body weights of humanised mice and human respectively

Extrapolated concentrations of caffeine in man were calculated using **Eq. 19**:

$$C_{Man\,(Extr)} = \frac{Dose_{Man}}{Dose_{Mouse}} * \frac{BW_{Mouse}^{d}}{BW_{Man}^{d}} * C_{Mouse}$$ **Eq. 19**

Where $C_{Man(Extr)}$ is a calculated caffeine concentration in man; $Dose_{Man}$ and $Dose_{Mouse}$ are caffeine doses in man (250 mg) and mice (0.164, 0.182 and 0.150 mg for hCYP1A1/1A2, Cyp1aKO and HRN mice respectively); BW_{Mouse} and BW_{Man} are mouse (0.0329, 0.0365 and 0.0299 kg for hCYP1A1/1A2, Cyp1aKO and HRN mice respectively) and human body weights respectively; d is slope of allometric plot for caffeine volume of distribution; C_{Mouse} is caffeine concentration in mice

Extrapolated values of blood collection time in man were calculated using **Eq. 20**:

$$t_{Man(Extr)} = t_{Mouse} * \frac{BW_{Man}^{d-b}}{BW_{Mouse}^{d-b}}$$ **Eq. 20**

Where $t_{Man(Extr)}$ is calculated time of blood collection in man; t_{Mouse} is time of blood collection in mice; BW_{Mouse} and BW_{Man} are mouse and human body weights respectively; d is a slope of allometric plot for caffeine volume of distribution; b is a slope of allometric plot for caffeine clearance

For caffeine pharmacokinetics in man the drug concentration at time of dosing was assumed to be equal to that in a pre-dose sample. The caffeine concentration in the

pre-dose sample measured in the placebo or fluvoxamine group was subtracted from every caffeine concentration measured post dose in the same experimental group.

Supplemental Scheme 1:

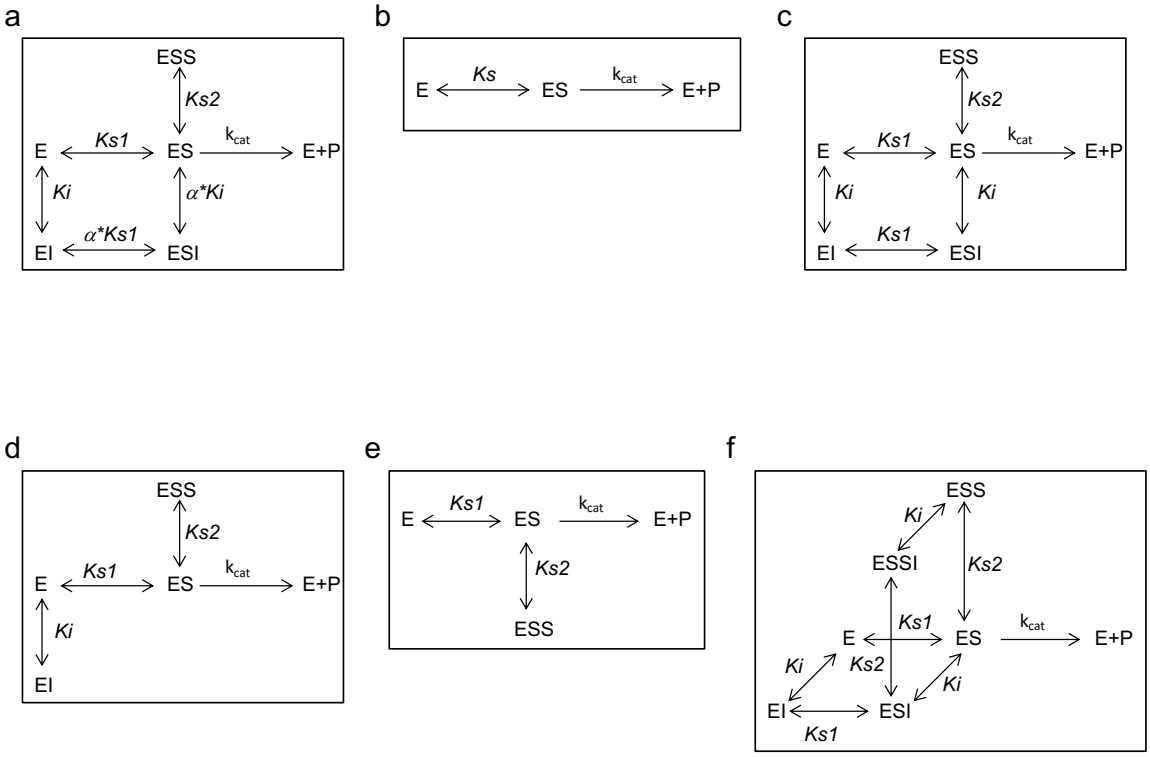

Supplemental Figure

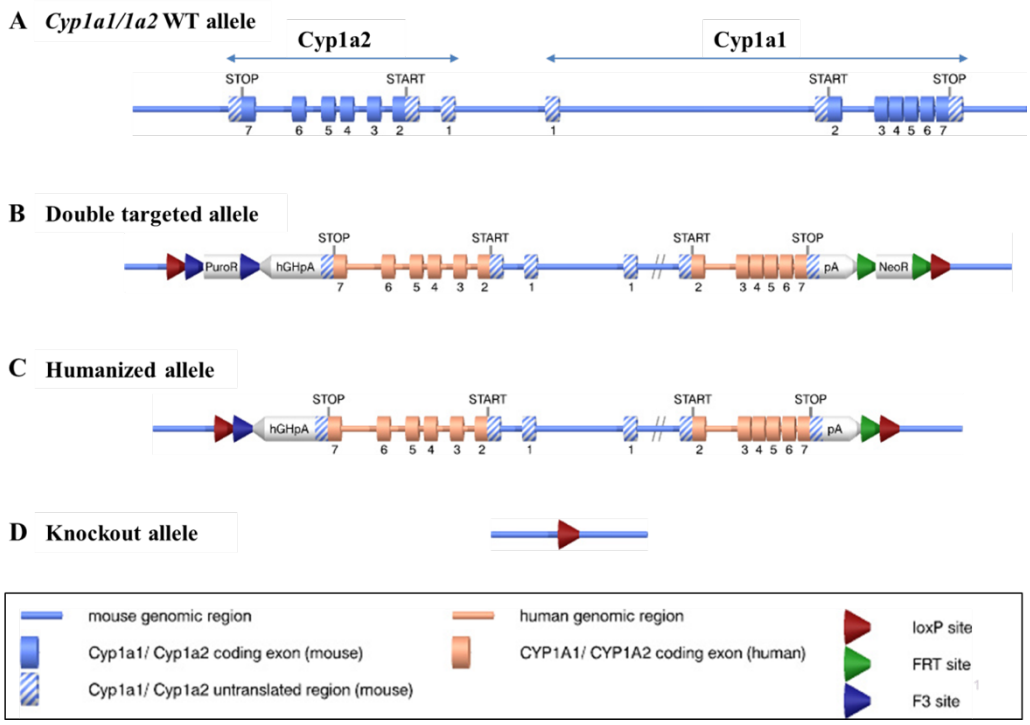

Supplemental Figure 1: Strategy to generate hCYP1A1/1A2 and Cyp1a KO mice

(**A**) Genomic organisation of the mouse *Cyp1a1/1a2* gene locus. The start ATGs and stop codons are shown. (**B**) Genomic organisation of *Cyp1a1/1a2* in targeted ES cells after homologous recombination. (**C)** *Cyp1a1/1a2* gene locus in the hCYP1A1/1A2 model after Flp-mediated deletion of the neomycin (NeoR) and puromycin (PuroR) expression cassettes. (**D**) *Cyp1a1/1a2* gene locus in the Cyp1a KO model after Cre-mediated deletion. For the sake of clarity sequences of the targeting vectors are not drawn to scale. pA = polyadenylation signal, hGHpA = polyadenylation signal of human growth hormone.

Supplemental Table

Supplemental Table 1: Body and liver weights

Data are mean ± SD; (% of mean of wild type of the same treatment group ± % SD); [% of mean of the same strain vehicle treated group ± % SD]; n=4;
* -Significantly different (unpaired t test (two tailed p values); * - p<0.05; ** - p<0.01)

Mouse line	Treatment	Body weight g	Liver weight g	Liver/Body weight ratio %
C57BL/6J	Corn oil	21.7±0.42 **(100±1.9)** **[100±1.9]**	1.15±0.08 **(100±6.8)** **[100±6.8]**	5.3±0.28 **(100±5.4)** **[100±5.4]**
	TCDD (10 mg/kg)	24.5±1.89 **(100±7.7)** **[113±8.7]***	1.30±0.08 **(100±6.3)** **[113±7.1]***	5.3±0.46 **(100±8.6)** **[101±8.7]**
hCYP1A1/1A2	Corn oil	21.8±4.24 **(100±19.5)** **[100±19.4]**	1.04±0.25 **(90±22)** **[100±24.3]**	4.7±0.36 **(89±6.8)*** **[100±7.6]**
	TCDD (10 mg/kg)	23.4±1.34 **(95±5.5)** **[107±6.1]**	1.15±0.11 **(88±8.3)** **[111±10.5]**	4.9±0.38 **(92±7.2)** **[104±8.1]**
Cyp1a KO	Corn oil	25.2±1.48 **(116±6.8)**** **[100±5.9]**	1.30±0.17 **(113±15)** **[100±13.3]**	5.1±0.41 **(97±7.8)** **[100±8.0]**
	TCDD (10 mg/kg)	26.2±0.89 **(107±3.6)** **[104±3.5]**	1.53±0.02 **(117±1.4)**** **[118±1.4]***	5.8±0.16 **(110±3)** **[114±3.1]***